arXiv:1408.5934v1 [astro-ph.SR] 25 Aug 2014

Lyman-α Observations of Astrospheres

Jeffrey L. Linsky

JILA, University of Colorado and NIST, Boulder CO, USA

jlinsky@jila.colorado.edu

Brian E. Wood

US Naval Research Laboratory, Washington DC, USA

brian.wood@nrl.navy.mil

ABSTRACT

Charge-exchange reactions between outflowing stellar wind protons and interstellar neutral hydrogen atoms entering a stellar astrosphere produce a region of piled-up-decelerated neutral hydrogen called the hydrogen wall. Absorption by this gas, which is observed in stellar Lyman-α emission lines, provides the only viable technique at this time for measuring the mass-loss rates of F–M dwarf stars. We describe this technique, present an alternative way for understanding the relation of mass-loss rate with X-ray emission, and identify several critical issues.

1. Introduction

The measurement of mass-loss rates for F–M dwarf stars and the development of theoretical models to predict these rates have challenged observers and theoreticians for many years. While *in situ* measurements of the solar-wind mass flux have been available since the early space age, such measurements are not feasible for other stars. Instead, Wood et al. (2005a,b) showed that astrospheric absorption in the stellar Lyman-α emission line provides a sensitive tool for measuring stellar mass-loss rates of late-type dwarf stars. Although other techniques have been proposed, including the search for charge-exchange-induced X-ray emission (Wargelin & Drake 2001) and free-free emission at radio wavelengths (Gaidos 2000; Fichtinger et al. 2013), the Lyman-α astrospheres technique is presently the only technique that provides credible results. We describe this technique in Section 2, present an alternative way for explaining the empirical relation of mass loss to X-ray flux in Section 3, and identify some critical issues in Section 4.

2. Lyman-α Observations of Astrospheres

The interaction of ionized stellar-wind plasma with inflowing, mostly neutral, interstellar gas leads to a rich phenomenology. Figure 1 shows an example of a hydrodynamic model of the

heliosphere computed by Müller & Zank (2004). The salient features of this model and other models of the heliosphere and astrospheres is the presence of a termination shock where the solar wind becomes subsonic, a heliopause/astropause that separates ionized solar/stellar wind plasma from charge-exchanged local interstellar medium (LISM) ions, and the so-called hydrogen wall where inflowing neutral hydrogen gas piles up, is decelerated, and is heated by the charge-exchange reactions. IBEX results (McComas et al. 2012) indicate that the inflow velocity of the LISM is likely too slow to produce a bow shock, however Scherer & Fichtner (2014) argue that inclusion of inflowing He^+ ions yields Alfvén and fast magnetosonic speeds slower than the inflow speed and thus a bow shock. As first predicted by Baranov & Malama (1993), hydrogen walls provide the observational basis for measuring stellar mass-loss rates. However, the small hydrogen column densities in these astrosphere regions, $\log N(HI)$ =14.0–15.0, means that optical depths in neutral metal lines also formed in these regions will be too small to detect, leaving Lyman-α as the only available spectral diagnostic for measuring stellar mass-loss rates.

Figure 2 shows the effect of neutral hydrogen absorption from the LISM and in the hydrogen walls of the star and the Sun on the Lyman-α emission line emitted by a star. Since the hydrogen wall gas is decelerated relative to the LISM gas, the solar hydrogen wall appears as extra absorption on the red side of the LISM absorption, and the stellar hydrogen wall viewed from outside of the star appears as extra absorption on the blue side of the LISM absorption. Figure 3 shows the effects of increasing stellar mass-loss rate on the stellar hydrogen-wall absorption computed with hydrodynamic astrosphere models (Wood et al. 2005a). This technique has been successfully applied to 15 stars or binary systems that are relatively close ($d < 32$ pc), with relatively small LISM neutral hydrogen column densities [$\log N(HI) < 18.5$]. Clearly, the LISM gas must contain a significant amount of neutral hydrogen for the development of a hydrogen wall and for this technique to work. Lyman-α observations of more stars are needed, but observational limitations will restrict the number of stellar winds that could be measured by this technique.

3. An Alternative Way for Explaining the Relationship of Mass loss and X-ray Flux

Wood et al. (2005a) proposed that the mass-loss rate per unit stellar surface area ($\dot{M}$) measurements for G and K dwarf stars shown in Fig. 4 can be fit by a power law, $\dot{M} \propto F_X^{1.34\pm0.18}$, for X-ray surface fluxes $F_X < 10^6$ erg cm^{-2} s^{-1}. While the fit looks good considering the roughly factor of two uncertainties in the mass-loss rate measurements and the varying X-ray fluxs that were measured at different times, there is no accepted explanation for this power-law relation. We therefore propose an alternative way of characterizing these data that suggests a physical scenario that could explain these results. We start by separating the data into three groups rather than by assuming a power-law relation.

Group 1 includes the Sun and four other stars (61 Vir, the unresolved binary α Cen AB, ϵ Ind, and 61 Cyg A). All of these stars are slow rotators (22–42 day periods), most have solar-like mass-loss rates (per unit surface area), $\dot{M}/\dot{M}_\odot \approx 1.0$, and F_X in the range 10^4–10^5 ergs cm^{-2} s^{-1}.

Cohen (2011), Wang (2010), and others have shown that the solar mass-loss rate is uncorrelated with F_X, although both $\dot{M}$ and F_X vary by over a factor of 10. The average solar mass loss rate ($\dot{M}_\odot \approx 2 \times 10^{-14} M_\odot$ yr^{-1}), however, is independent of F_X despite the very different number of active regions on the solar disk at times of solar activity minima and maxima.

Group 2 consists of two stars and two unresolved binary systems with F_X in the narrow range 3–5$\times 10^5$ ergs cm^{-2} s^{-1}. The two stars (ϵ Eri and ξ Boo B) are moderate speed rotators ($P_{\rm rot}$=11.68 and 11.5 days, respectively). The other two targets are unresolved binaries (70 Oph AB and 36 Oph AB) with rotational periods in the range 19.7–22.9 days and measured mass-loss rates only for the binary systems rather than for the individual stars.

The third group of G–K dwarf stars consists of π^1 UMa (Wood et al. 2014) and ξ Boo A (Wood & Linsky 2010). These stars are rapid rotators ($P_{\rm rot}$ = 4.69 and 6.2 days, respectively), have large $F_X \approx 2 \times 10^6$ ergs cm^{-2} s^{-1}, but small mass-loss rates similar to the Sun. We note that these mass-loss rates are a factor of 100 times smaller than theoretical estimates for π^1 UMa (Cranmer & Saar 2011; Drake et al. 2013) and for τ Boo, an F7 V star with $P_{\rm rot}$ = 3.0 days (Vidotto et al. 2012).

The very different behavior between mass loss, which emerges only along open magnetic-field lines, and X-ray flux, which is emitted mostly in closed magnetic-field regions with high electron densities, likely depends on the energy available for driving mass loss at the coronal base of open field lines, the number of open field lines, and the divergence of the open field lines with height in the corona. While detailed theoretical studies of wind acceleration mechanisms (e.g., Holzwarth & Jardine 2007; Cranmer & Saar 2011) and coronal magnetic-field morphologies (e.g., Jardine et al. 2013) are needed, we outline here a simple physical model that may explain the complex relationship between $\dot{M}$ and F_X shown in Fig. 4.

Wang (2010) showed that for the Sun, the mass flux along an open magnetic-field line is proportional to the magnetic-field strength at its coronal base footpoint. Since the coronal base magnetic-field strength near active regions is much larger than for high-latitude coronal holes, the mass flux in field lines located near active regions is much larger than for open field regions away from active regions (e.g., polar holes). However, the divergence of field lines emerging from near active regions is much larger than for open field regions away from active regions. As a result, the greater divergence of field lines from active regions compensates for the larger mass flux in these field lines leading to the same average solar mass-loss rate even when the surface coverage of active regions changes as indicated by a factor of 10 range in F_X. This explanation for the nearly constant value of $\dot{M}$ over at least a factor of 10 range in F_X seen in the solar data likely also explains the results for the other Group 1 stars.

For the faster rotating stars in Group 2, especially ϵ Eri and ξ Boo B, the much stronger magnetic dynamo produces much larger magnetic fluxes (Reiners 2012). This likely means that more active regions are distributed across their stellar surfaces and stronger magnetic-field strengths outside of these active regions are present in the Group 2 stars compared with the Group 1 stars.

As a result, the coronal surface area not covered by active regions is decreased substantially such that there is much less available volume for open field lines to expand. The smaller divergence of field lines from active regions will not be able to compensate for the enhanced mass flux along these stronger magnetic-field lines. Cohen (2011) showed that in the absence of significant magnetic-field divergence, stellar mass-loss rates will increase with the magnetic field strength and the available energy at the base of the magnetic field lines.

A viable explanation for the solar-like mass-loss rates for the rapidly rotating stars in Group 3 is a matter of speculation at this time. We suggest that the very strong dynamos in these stars produce complex magnetic-field morphologies including a strong toroidal component seen in rapidly rotating stars like ξ Boo A (Petit et al. 2005). These very strong magnetic fields are likely closed in very active stellar coronae leaving only a few open-field lines from which the stellar wind can emerge. The fewer open-field lines could more than compensate for the stronger mass-flux rates in the remaining open-field lines.

Simulations by Suzuki et al. (2013) of MHD wave propagation upwards along open magnetic field lines from the photospheres of solar-like stars may explain the empirical correlation of $\dot{M}$ with F_X shown in Figure 4. They found that with increasing magnetic field strength and turbulence in the photosphere (the origin of stellar activity), the reflection of upwardly propagating Alfvén waves is less efficient, leading to an increase in the energy available in the corona for mass loss and X-ray emission. However, radiative losses in the chromosphere increase even faster than the mass-loss flux, leading first to $\dot{M}$ saturation at a high level and then to decreasing $\dot{M}$ with increasing F_X. Qualitatively, this may explain the increase and then decrease of $\dot{M}$ with increasing F_X, but the peak $\dot{M}$ corresponding to saturation in these calculations is much larger than is observed and the decrease in $\dot{M}$ at very large F_X levels was not modeled in detail.

4. Critical Issues

The study of cool dwarf star astrospheres has made important progress from the early theoretical models of the heliosphere that first showed the presence of a hydrogen wall (Baranov & Malama 1993), through the development of sophisticated-hydrodynamic models of stellar atmospheres by Müller, Izmodenov, Zank, and others, to the testing and refinement of these models by comparison with stellar Lyman-α observations. Despite this important progress, there remain a number of critical problems requiring future theoretical and observational studies:

Charge-exchange rates The existence and physical properties of solar/stellar hydrogen walls depend critically on charge-exchange reaction rates between outflowing solar/stellar wind ions (primarily protons) and the inflowing LISM neutral hydrogen atoms. If the presently assumed charge-exchange reactions rates are in error, then the inferred values for N(H I), heating, and deceleration of neutral hydrogen atoms in the hydrogen wall will also be in error. It is important to compute charge-exchange reaction rates for the low densities and

likely non-Maxwellian velocity distributions of the interacting species.

Proper inclusion of neutrals Neutral hydrogen and helium atoms inflowing from the LISM have long mean-free paths that are not easily included in hydrodynamic model calculations. The neutrals must be treated with kinetic equations or Monte Carlo simulations that must be coupled somehow to the hydrodynamic calculations for the plasma.

Theoretical models of stellar astrospheres may not include all physical processes For example, most models and simulations assume that stellar mass loss is constant or quasi-steady state and, therefore, do not include transient events like coronal mass ejections (CMEs) that are seen on the Sun but not yet detected on stars. Drake et al. (2013) argued that CMEs in active stars could dominate the mass-loss rate based on an extrapolation of solar data, but this process must be tested in realistic models and against stellar CME measurements when they become available. The magnetic field morphology, in particular the height at which closed field lines open, plays an important role in mass loss. Realistic models should compute the magnetic field structure self-consistently with the mass outflow.

Accurate boundary conditions Whether the LISM gas flowing into the heliosphere forms a bow shock or a bow wave requires accurate values for the interstellar gas flow speed and magnetic field strength. Even for the Sun, for which we have the best data, these quantities are not yet known accurately. In particular, the magnetic field strength outside of the heliopause has not yet been measured by the Voyager spacecraft or reliably estimated. For nearby stars, the flow speed of the star with respect to the interstellar medium gas is probably uncertain by less than 3 km s^{-1}, but the interstellar magnetic field is not well known. Thus the presence or absence of a bow shock is not known in many cases. A critical question is whether the interstellar gas flowing into an astrosphere is partially ionized like the LIC or fully ionized. In the latter case, there will be an astrosphere but no hydrogen wall and thus no possibility for measuring the mass-loss rate. The presence of Lyman-α absorption on the short wavelength side of the interstellar absorption indicates the presence of a hydrogen wall and that the star is surrounded by partially ionized interstellar gas, but the inferred value of $\dot{M}$ depends on the neutral hydrogen number density of the inflowing gas which has been assumed to be the same as in the LIC given the absence of other measurements. The nondetection of astrospheric Lyman-α absorption can be explained either by assuming that the star is embedded in fully-ionized interstellar gas or that the star has an extremely low mass-loss rate. The latter is unlikely but cannot be ruled out at this time.

Active stars appear to have low mass-loss rates We have suggested that the low mass-loss rates for the two rapidly rotating stars with $F_X > 10^6$ ergs cm^{-2} s^{-1} result from very strong magnetic fields with complex geometries that severely restrict the number of open field lines in the corona. A new generation of theoretical models is needed to test and develop this scenario. There are models for very rapidly rotating stars in which magnetocentrifugal acceleration is important (Vidotto et al. 2011) and for T Tauri stars for which accretion and

disk winds are important (e.g., Vidotto et al. 2010). What is lacking are models for stars like π^1 Ori and ξ Boo A, which are active stars without extreme rotation or T Tauri-like phenomena. Numerical simulations of MHD wave propagation in open flux tubes embedded in realistic atmospheres such as those of Suzuki et al. (2013), Cranmer & Saar (2011), and Holzwarth & Jardine (2007) provide insight into the essential physics and need to be developed further. Observations of more stars, especially those with F_X near and above 10^6 erg cm^{-2} s^{-1}, are also needed to determine whether the decrease in $\dot{M}$ for $F_X \geq 10^6$ erg cm^{-2} s^{-1} is sharp or gradual, or indeed typical. Also, reobservations of stellar Lyman-α lines 5–10 years after the original observations would test whether astrospheres and mass-loss rates change during the time scale for stellar winds to propagate well out into their astrospheres.

5. Conclusions

The study of astrospheres is intimately connected with the measurements of stellar-wind mass fluxes for late-type stars. At present the Lyman-α astrospheres technique is the only successful technique for infering these mass-loss rates. New theoretical models for stellar astrospheres and stellar mass loss are needed to explain in physical terms the results provided by this technique.

JL acknowledges support by the Space Telescope Science Institute (STScI) to the University of Colorado for HST observing program GO-11687. BW acknowledges support by STScI for observing program GO-12596. STScI is operated by the Association of Universities for Research in Astronomy, Inc. under NASA contract NAS 5-26555. We thank the referees for their very useful comments.

REFERENCES

Baranov, V.B. & Malama, Y.G. 1993, JGR, 98, 15,157

Cohen, O. 2011, MNRAS, 417, 2592

Cranmer, S.R., & Saar, S.H. 2011, ApJ, 741, 54

Drake, J.J., Cohen, O., Yashiro, S., & Gopalswamy, N. 2013, ApJ, 764, 170

Fichtinger, B., Güdel, M., Hallinan, G., Mutel, R., Lynch, C., Skinner, S., Gaidos, E., & the PAH collaboration 2013, Protostars & Planets VI, poster #1K098

Gaidos, E.J., Güdel, M., & Blake, G.A. 2000, Geophys. Res. Lett., 27, 501

Holzwarth, V., & Jardine, M. 2007, A&A 463, 11

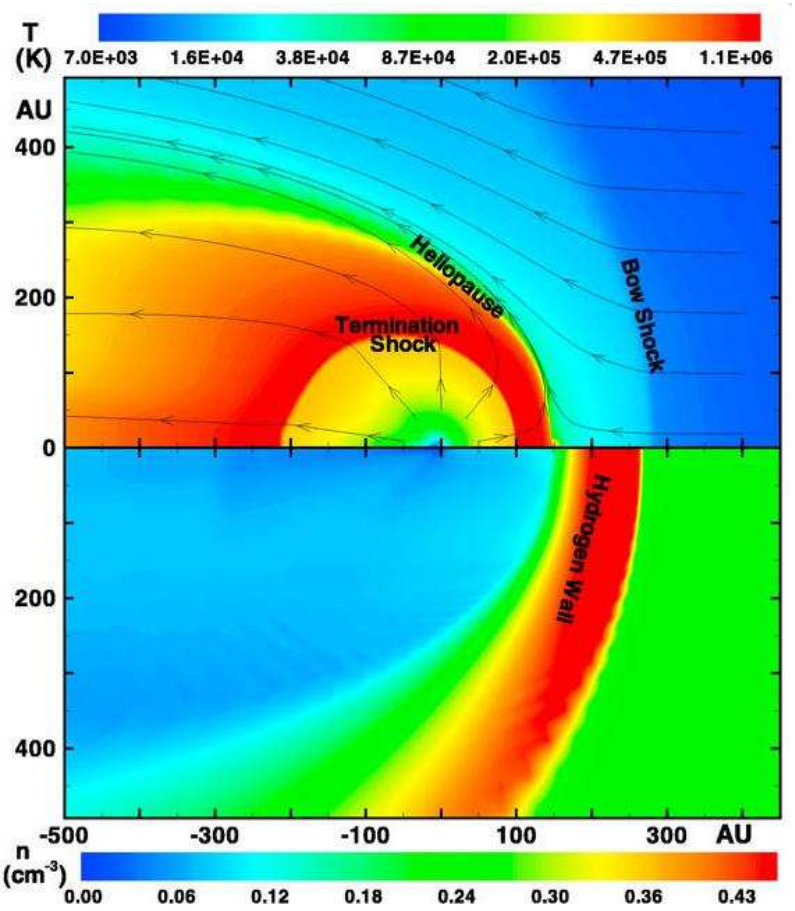

Fig. 1.— This figure shows the different components of a heliosphere/astrosphere as seen in temperature (top) and neutral hydrogen density (bottom). At the termination shock, the supersonic solar/stellar wind becomes subsonic and heats the postshock gas. Further out from the Sun/star, the heliopause/astropause separates the outflowing-ionized solar/stellar wind gas from the interstellar gas that has been ionized by charge exchange reactions. The pile-up of heated and decelerated neutral hydrogen gas at larger distances also results from charge exchange reactions with the outflowing solar/stellar wind ions. Beyond the hydrogen wall, there may be a bow shock depending on the inflow speed of interstellar gas and its magnetic field strength. Figure from Müller & Zank (2004).

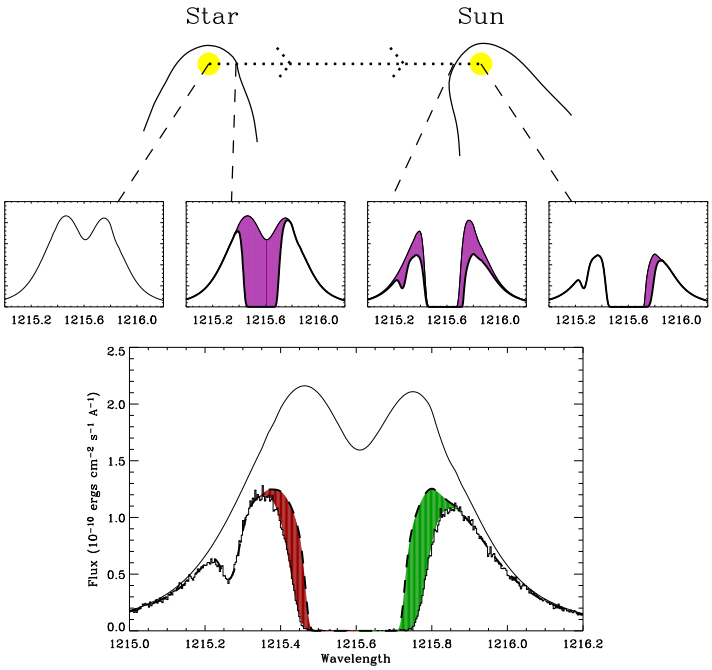

Fig. 2.— The presence of absorption components in the observed stellar Lyman-α emission line (bottom) is illustrated in this schematic sketch of the journey of Lyman-α photons from the star to an observer inside the heliosphere (Wood 2004). Astrospheric absorption is blue-shifted relative to the line of sight component of the interstellar flow velocity because the stellar hydrogen-wall gas is decelerated (in the stellar reference frame) relative to the interstellar medium flow. Lyman-α photons then traverse the LISM and are absorbed by interstellar neutral hydrogen at the projected flow velocity of the LISM. The hydrogen wall gas in the heliosphere produces redshifted absorption as a result of its deceleration relative to the interstellar gas. The effect of these three absorption components (illustrated in the middle plots) is to produce extra absorption on the blue side of the LISM absorption indicating the presence of a hydrogen wall surrounding the star, and absorption on the red side of the LISM feature produced by the solar hydrogen wall.

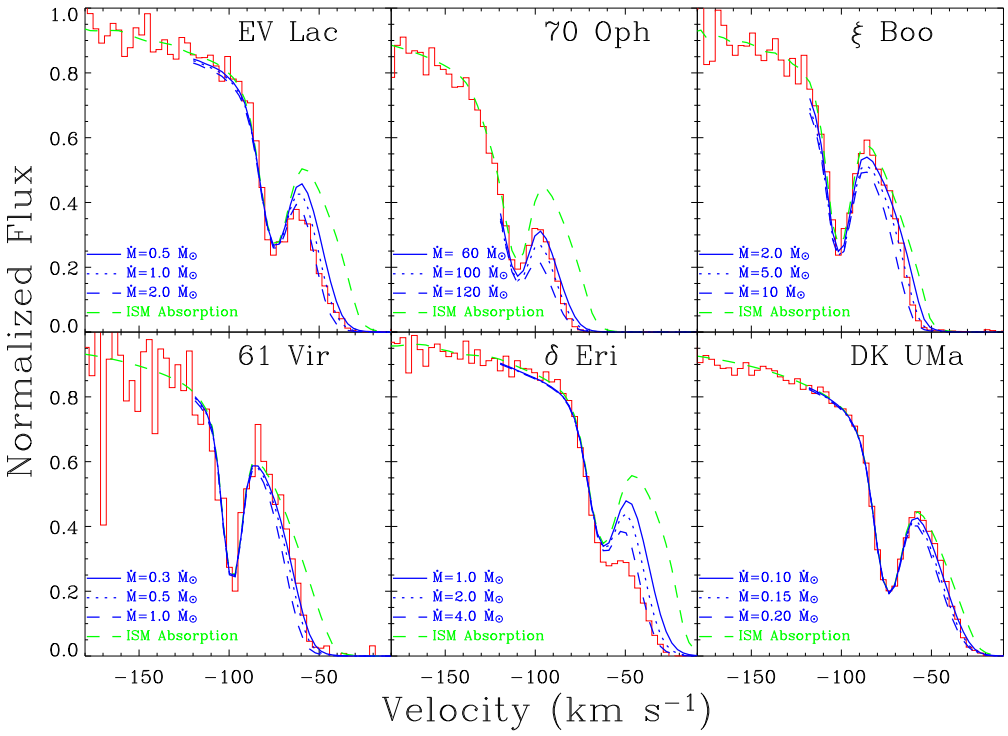

Fig. 3.— Comparisons of the observed absorption on the short wavelength side of the Lyman-α lines of six stars with hydrodynamic models assuming wind speeds of 400 km s^{-1} and parameters of the LISM (Wood et al. 2005a). The effect of increasing stellar-wind mass flux is to increase the amount of blue-shifted absorption by the stellar hydrogen wall (in units of the solar mass loss rate $\dot{M} = 2 \times 10^{-14}$ solar mass per year). The absorption line centered near -80 km s^{-1} is deuterium Lyman-α absorption in the LISM.

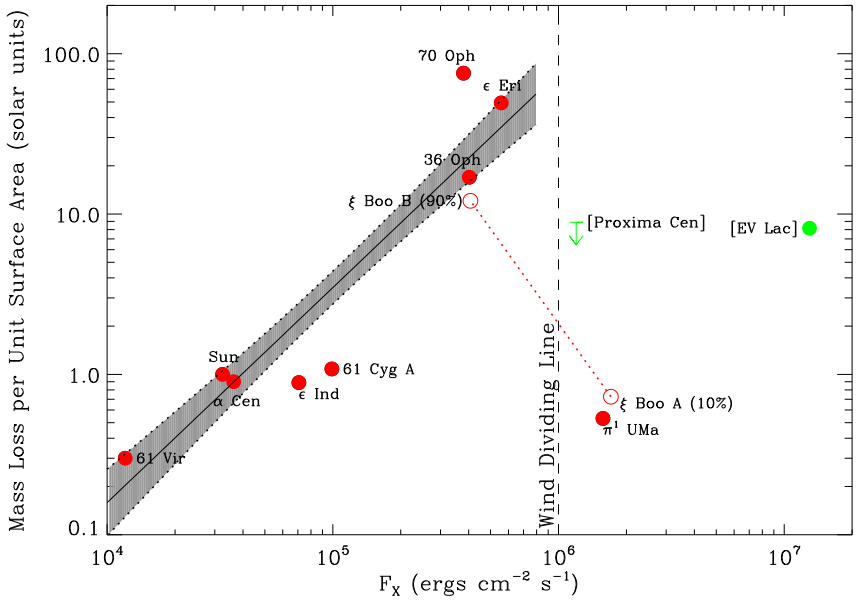

Fig. 4.— A plot of mass loss rate with respect to x-ray flux, both quantities expressed per unit stellar surface area. For stars with x-ray surface fluxes less than 10^6 erg cm^{-2} s^{-1}, there is a power law relation comparing mass flux rate to x-ray flux. This simple relation does not hold for stars with larger F_X including the young star π^1 UMa, ξ Boo A, and the M dwarf flare stars Proxima Centauri and EV Lac (Wood et al. 2014).

Jardine, M., Vidotto, A.A., van Ballegooijen, A., Donati, J.-F., Morin, J., Fares, R., & Gombosi, T.I. 2013, MNRAS, 431, 528

McComas, D.J., et al. 2012, Science, 336, 1291

Müller, H.-R. & Zank, G.P. 2004, JGR, 109, A7

Petit, P. et al. 2005, MNRAS, 361, 837

Reiners, A. 2012, Living Rev. Solar Phys., 8, 1

Scherer, K. & Fichtner, H. 2014, ApJ, 782, 25

Suzuki, T. K., Imada, S., Kataoka, R., Kato, Y., Matsumoto, T., Miyahara, H., & Tsuneta, S. 2013, PASJ, 65, 98

Vidotto, A.A., Fares, R., Jardine, M., Donati, J.-F., Opher, M., Moutou, C., Catala, C., & Gombosi, T.I. 2012, MNRAS, 423, 3285

Vidotto, A.A., Jardine, M., Opher, M., Donati, J.-F. & Gombosi, Y.I. 2011, MNRAS, 412, 351

Vidotto, A.A., Opher, M., Jatenco-Pereira, V., & Gombosi, T.I. 2010, MNRAS, 720, 1262

Wang, Y,-M. 2010, ApJ, 715, L121

Wargelin, B.J. & Drake, J.J. 2001, ApJ, 546, 57

Wood, B.E. 2004, Living Rev. Solar Phys. 1, 2

Wood, B.E., & Linsky, J.L. 2010, ApJ, 717, 1279

Wood, B.E., Müller, H.-R., Redfield, S. and Edelman, E. 2014, ApJ, 781, 33

Wood, B.E., Müller, H.-R., Zank, G.P., Linsky, J.L., and Redfield, S. 2005a, ApJL, 628, L143

Wood, B.E., Redfield, S., Linsky, J.L., Müller, H.-R., and Zank, G.P. 2005b, ApJS, 159, 118

This preprint was prepared with the AAS LaTeX macros v5.2.